

## Research article



# A comparative study on electrochemical performance of KOH activated carbons derived from different biomass sources - *Musa acuminata* stem, *Pongamia pinnata* seed oil extract cake, *cajanus cajan* stem and *Asclepias syriaca* floss

Gopalakrishna Byatarayappa<sup>a</sup>, Radhika M. G<sup>b</sup>, Srilakshmi R<sup>c</sup>, Tejashree V<sup>a</sup>,  
Krishna Venkatesh<sup>a</sup>, Nagaraju N<sup>d</sup>, Kathyayini Nagaraju<sup>a,\*</sup>

<sup>a</sup> Centre for Incubation Innovation Research and Consultancy (CIIRC), Jyothy Institute of Technology, Tataguni, off Kanakapura Road, Bengaluru, 560082, Karnataka, India

<sup>b</sup> Department of Physics, R.V. College of Engineering, Bengaluru, 560059, Karnataka, India

<sup>c</sup> Department of Electronics and Communications, Jyothy Institute of Technology, Tataguni, off Kanakapura Road, Bengaluru, 560082, Karnataka, India

<sup>d</sup> Department of Chemistry, St. Joseph's College P.G. Centre, 36, Langford Road, Shanthinagar, Bengaluru, 560027, Karnataka, India

## ARTICLE INFO

## Keywords:

Biomass  
Activated carbon  
Surface properties  
Supercapacitors  
Cycles stability

## ABSTRACT

In the present scenario of research, the recycling of inexpensive widely available agricultural waste/biowaste to activate carbon (AC) and procurement of value-added product has significant impact on energy storage systems, particularly in Electrochemical double layer capacitors (EDLCs). Herein, we report the production of KOH activated carbons from different biomass sources such as *Musa Acuminata* stem (MAC), *Pongamia pinnata* seed oil extract cake (PPC), *Cajanus Cajan* stem (CCC) and *Asclepias syriaca* floss (ASC) for the said purpose. Initially, the biomass materials were pyrolyzed at 550 °C and then activated with KOH at 800 °C. All the carbon materials were characterized for their physico-chemical properties by various analytical techniques and compared. Further, these materials were studied for their electrochemical performance using suitable electro-analytical techniques in 1 M KOH solution. ACs (Activated carbons) derived from MAC, PPC, CCC & ASC were estimated in three electrode system and were found to exhibit a specific capacitance (Cs) of 358, 343, 355 & 540 F/g at a scan rate of 2 mV/s and 102, 188, 253 & 256 F/g at a current density of 2.5 A/g respectively. The main novel objective of this work is to correlate the morphological and surface properties of these ACs obtained from different biomass sources with electrochemical performance. A symmetric coin cell constructed with ASC material exhibited Cs of 67 F/g at a current density of 2.5 A/g with maximum energy & power densities (ED & PD) of 37.2 W h/kg and 19.9 kW/kg respectively. Further the cell showed 25,000 cycles stability with 86% Cs retention and 100% coulombic efficiency.

\* Corresponding author.

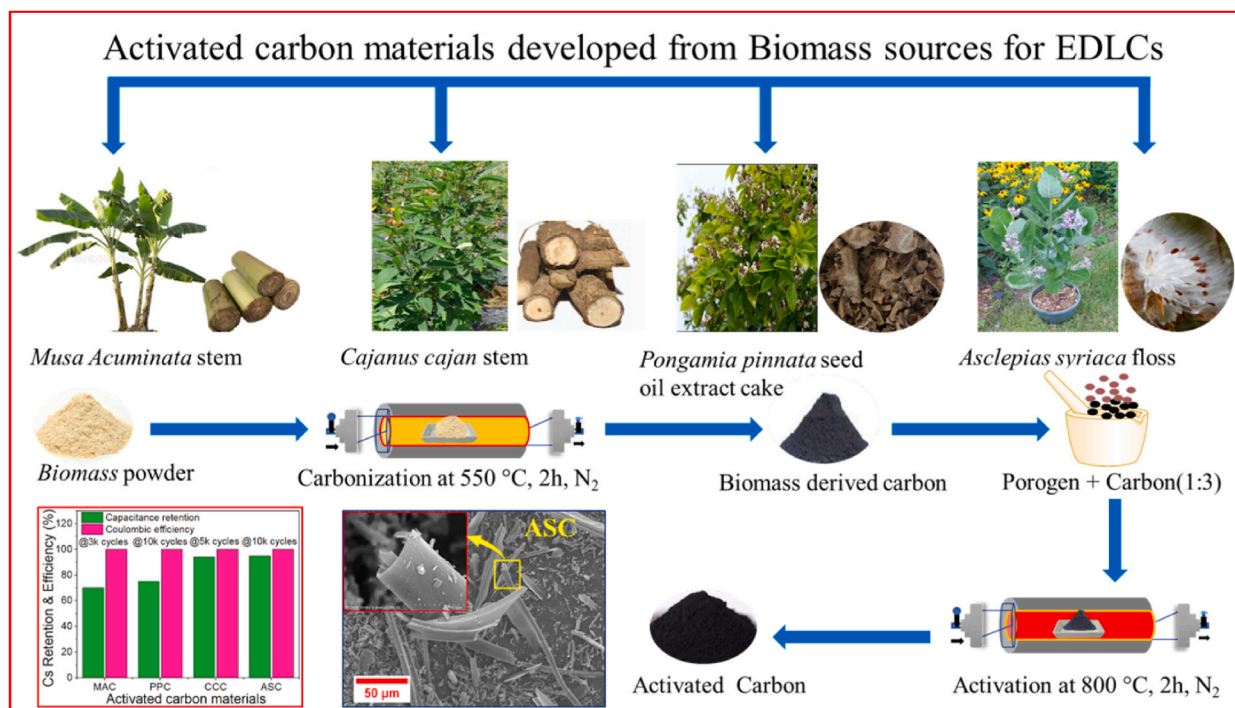
E-mail address: [nkathyayini45@gmail.com](mailto:nkathyayini45@gmail.com) (K. Nagaraju).

## 1. Introduction

Recycling of low-cost and widely available biomass to value added materials as well as products is a promising field of research. Activated carbons derived from such biomass finds vital applications in the field of fuel cells, batteries and more prominently supercapacitor electrode materials as Electrochemical double layer capacitors (EDLCs). This is predominantly owing to distinctive properties like specific surface area, pore volume, good conductivity, chemical resistance, and desirable pore size exhibited by ACs derived from biomass sources [1–3]. Hence the development of “Green” carbon for various hybrid supercapacitors (associated with Sodium, Potassium, Lithium & Zinc ions) are widely used in “Green” energy equipment’s is an encouraging area of electrochemical research [4]. There are mainly four kinds of energy storage and conversion devices which are commonly used for commercial applications. These are capacitors, supercapacitors, batteries and fuel cells [5]. Supercapacitors/Ultracapacitors are new energy storage devices that are intermediate between batteries and capacitors according to their energy density (ED) and power density (PD) generated by these energy storage systems [5–7].

The dominance of supercapacitors on batteries and fuel cells are due to high specific power (100–104 W/kg), longer cycles stability (nearly  $5 \times 10^5$ ) with good specific capacitance (Cs) retention, low internal resistance, wide operating temperature range between  $-40^\circ\text{C}$  to  $70^\circ\text{C}$  and low maintenance. Further heavy metals and other hazardous chemicals are not used as electrode materials in supercapacitors, thus protecting environment and forms “Green” energy storage system. Hence, the development of electrode materials for supercapacitors is a favorable research area compared to other energy storage devices. The charge storage in supercapacitor is due to gathering of charges via adsorption/desorption as in EDLCs or reversible redox reaction as in Pseudocapacitors (PCs), and combination of these would lead to hybrid supercapacitors [8–10]. In Pseudocapacitors (examples metal oxide/s & conducting polymers), a fast reversible redox reaction generates and store electrical charges [11–19]. Even though, the estimated Cs values in PCs are higher than EDLC’s, there are also some disadvantages in PCs. The main disadvantages of pseudocapacitors includes i) poor electrical conduction ii) poor cyclability iii) narrow operating potential window [14]. In EDLC’s (examples activated carbon, carbon black, carbon nanotubes, carbon aerogels, graphene oxide, and reduced graphene oxide) charge storage is by adsorption/desorption at the interface between electrode surface and electrolyte [20–22]. Among various EDLC’s carbon materials derived biomass are significant as they are inexpensive, easily & abundantly available with good chemical stability & environmental adaptability. Biomasses such as plants, animals, microorganisms & metabolites are rich in organic matter and are good precursor for obtaining porous activated carbon [23–27].

Currently there are mainly three activation procedures that are followed such as physical, chemical and physico-chemical; however there are some pros and cons of these individual process. The main drawback of physical activation is that the process needs high temperature and no control over the porosity of activated carbon. The benefits of chemical activation include low temperature & short duration process, high carbon content, controlled porosity and leads to high surface area carbon material [28]. There are various porogens used in chemical activation such as alkaline, acidic and neutral. However as mentioned in our previous work, KOH is



**Scheme 1.** Synthesis of Activated carbons from various biomass sources.

universal porogen used as chemical activation and has several aids. Chemical activation using KOH suppresses tar generation, low temperature activation, non-carbon constituents are removed, and formation of desired high surface area carbon. KOH interacts with carbon undergoes some reactions and finally becomes activated carbon which finds several applications in various fields [29–31].

In chemical activation high surface area and desired porosity can be obtained by varying the temperature, duration of the process, impregnation ratio of carbon, flow rate of inert gas and nature of porogen. Based on these synthesis parameters, conversion of biomass into activated carbon was studied earlier in detail [32–34]. In this research article, we have made comparison of electrochemical properties of KOH activated carbons derived from four different biomasses such as *Musa Acuminata* stem (MAC), *Pongamia pinnata* (PPC) seed oil extract, *Cajanus cajan* (CCC) stems and *Asclepias syriaca* (ASC) floss (Scheme 1). Here the influence of morphological properties and their surface properties on electrochemical performance of EDLCs are studied. The schematic representation of the research work carried out in this article is as follows.

## 2. Materials and methods

### 2.1. Materials

Four different biomasses such as *Musa Acuminata* stem (MAC), *Pongamia pinnata* seed oil extract (PPC), *Cajanus cajan* (CCC) stems and *Asclepias syriaca* (ASC) floss were collected in and around our campus, Bangalore. The chemicals used in this research work were Potassium hydroxide (KOH), Hydrochloric acid (HCl), Polyvinyl di-fluoride (PVDF), Iso-propyl alcohol (IPA) and *N*-Methylpyrrolidone (NMP) of analytical grade were procured from commercial sources.

### 2.2. Preparation of activated carbon from various biomasses

Initially four different biomasses were washed with plenty of water to remove earthy materials and were dried in a hot air oven for overnight at 110 °C. In our earlier work, we have optimized the carbonization conditions and chemical activation using KOH and the same was followed [32]. In a typical synthesis procedure, the dried samples were carbonized separately at 550 °C for 2 h in N<sub>2</sub> atmosphere with flow rate of 100 mL/min at a heating rate of 10 °C/min in a horizontal furnace. About 60–70% yields of black solid carbon material were obtained in each carbonization process. The carbon materials were individually activated with KOH by mixing calculated amounts of carbon from respective biomass and KOH pellets in the ratio 1:3 in a ceramic crucible with small quantities of water and left overnight in hot air oven at 110 °C. The resulting substances were activated at 800 °C for 2 h under N<sub>2</sub> atmosphere (100 mL/min) in a horizontal furnace during separate chemical activation process. In our earlier studies, we have proved that chemical activation of carbon derived from biomass materials at 800 °C proved better interaction of KOH (Vaporizes at 762 °C) with carbon material by improving the surface properties [30,33,34]. These four activated carbon materials were cooled to room temperature and separately washed with 3 M HCl to reduce excess and physically adsorbed KOH. Finally, activated carbon materials were washed with sufficient amount of water to reach neutral pH of the filtrate and the residues were individually dried at 110 °C overnight in a hot air oven.

### 2.3. Characterization of carbon materials

All the four carbon materials derived from different biomass were characterized by suitable analytical techniques such as Powder X-ray diffraction (*P*-XRD), Raman spectroscopy, Brunner Emmett Teller (BET) surface area, Scanning Electron Microscopy (SEM) and Energy Dispersive Spectroscopy (EDS) to evaluate their physico-chemical properties. *P*-XRD patterns were obtained on Bruker X-ray diffractometer with Cu K<sub>α</sub> radiation ( $\lambda = 0.154$  nm) in a  $2\theta$  range of 10° to 80° at 40 kV and 2° min<sup>-1</sup> scanning rate. Raman spectra of carbon materials were recorded on EN Wave optronics ez Raman pro using green laser beam (532 nm). BET surface areas of the carbon materials were determined under N<sub>2</sub> adsorption-desorption and the data was acquired using BELSORP Max instrument at liquid N<sub>2</sub> temperature. Before the N<sub>2</sub> adsorption-desorption measurements, all the carbon samples were degassed under vacuum for 16 h at 200 °C. SEM images and EDS for elemental composition of all the carbon materials were acquired on Hitachi SU 3500.

### 2.4. Electrochemical studies in a three-electrode system

The electrochemical characterization of MAC, PPC, CCC and ASC-carbon materials were initially performed in a three-electrode system comprising of platinum wire (counter electrode), saturated calomel electrode (SCE) (reference electrode) and the working electrode in 1 M KOH electrolyte using CHI 660 E electrochemical workstation. The working electrode was fabricated by mixing active carbon material (85%), Ketjen black (10%-EC 600JD) binder (5%-PVDF) and made into slurry using a few drops of NMP solvent. The thick slurry thus obtained was coated on a 1 cm<sup>2</sup> Toray carbon paper & vacuum dried at 80 °C for 12 h and electrochemical studies were scrutinized using electrochemical workstation CHI660E. The three crucial electrochemical techniques, i) cyclic voltammetry (CV) were carried out at various scan rates, ii) chronopotentiometry (CP) at different current densities and iii) Electrochemical Impedance spectroscopy (EIS) to evaluate their non-faradaic behaviour as well as cycle stability. EIS studies were accomplished at an open circuit potential (OCP) by applying a sinusoidal alternating voltage frequency in the range of 10<sup>-2</sup> to 10<sup>5</sup> Hz at amplitude of 5 mV [11]. The electrochemical performance with respect to Cs, ED, PD and coulombic efficiency of all activated carbons were calculated using standard equations by CV, CP and EIS studies [32].

## 2.5. Fabrication of symmetric supercapacitor device- (coin cell-CR2032)

The supercapacitance performance of KOH activated carbons derived from four different biomasses were initially checked by routine CV, CP and EIS analysis in three-electrode system and the results are further discussed in the text. Interestingly, ASC material exhibited high supercapacitance performance in 1 M KOH solution in all the three techniques (section 3.2). Henceforward, ASC material was selected to design a traditional symmetric Swagelok-type coin cell (CR-2032) in 1 M KOH solution. To fabricate this cell, graphite felt was utilised as current collector and initially cleaned with ethanol solution using ultrasonicator for 1 h with 200 W power & 42 KHz frequency and then dried in a hot air oven at 80 °C for 4 h. 2.5 mg of ASC carbon slurry (preparation as described in section 2.4) was coated on each of the two circular shaped (diameter-12 mm) graphite felt electrodes and dried for 12 h at room temperature. Whatman-41 filter paper (separator) was soaked with few drops of 1 M KOH and sandwiched between the two electrodes using a mechanical crimping machine by imposing a pressure of one ton while designing the coin cell (JES). The supercapacitance performance of this cell was further examined by CV, CP, EIS and cycle stability using CHI 660 E electrochemical workstation. The EDLC parameters such as, Cs, ED, PD, coulombic efficiency and capacitance retention of the coin cell were estimated as mentioned in our earlier work [10].

## 3. Results and discussion

### 3.1. P-XRD, Raman, BET and SEM analysis

All the activated carbon materials derived from four different biomasses were analyzed by powder X-ray diffraction technique. The diffraction patterns obtained for activated carbons are provided in Fig. 1a. It was noticed that all the activated carbon materials did not exhibit same kind of crystallinity. Amongst all the activated carbons derived from various biomasses, PPC was more crystalline and MAC was more amorphous. In carbon samples (PPC, CCC & ASC), two main broad diffraction patterns were observed around 2 $\theta$  between 20° to 35° and 43° corresponds to (002) and (100) planes representing amorphous graphitic plane with different intensities and shift in peak positions [32,35,36]. Interestingly PPC exhibits higher degree of crystallization and a broad graphitic peak in the range 20° to 30° as well as sharp peaks in the same range. However in MAC, such significant diffraction peak was not observed but the material seems to be more amorphous. It is noteworthy to mention here that, a common and an efficient porogen KOH with same chemical activation conditions was used in the synthesis of these activated carbons, during activation process interaction of KOH with

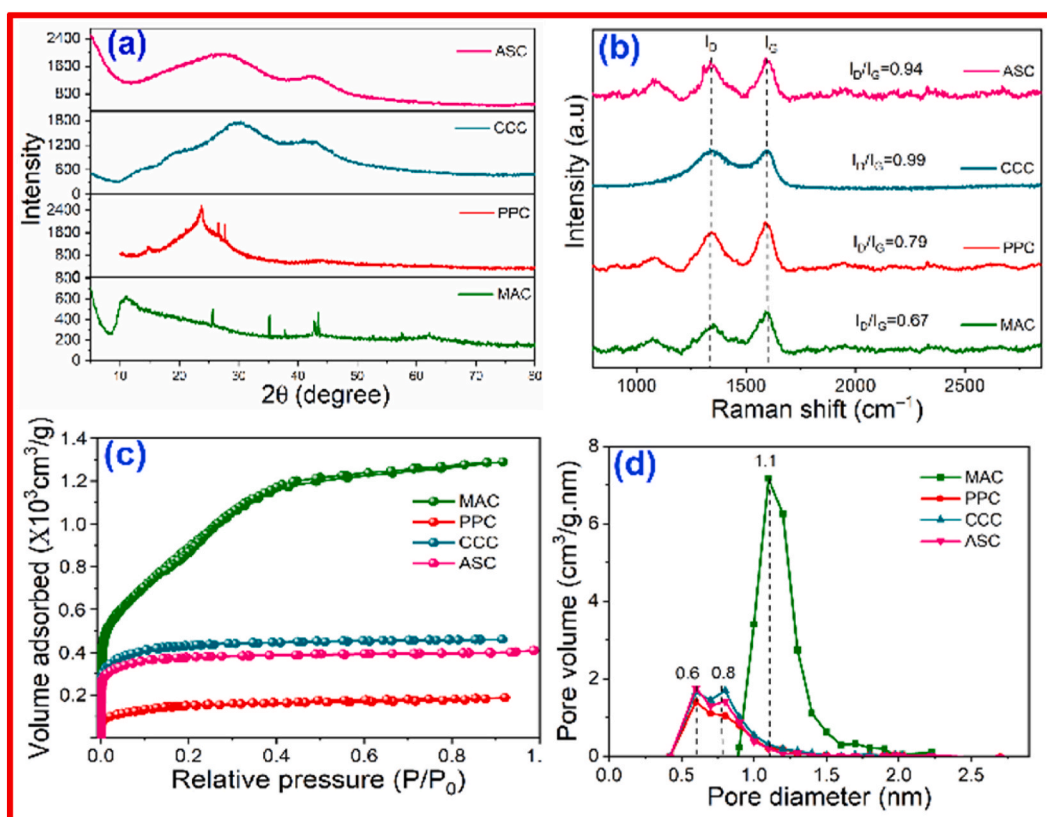


Fig. 1. (a) P-XRD patterns (b) Raman spectra (c) N<sub>2</sub> adsorption and desorption isotherms and (d) Micropore plot of all carbon materials.

carbons derived from different biomasses were entirely different. The difference in X-ray diffraction patterns of carbon materials may be attributed to the different percentage of constituents of biomass such as 67.97%, 20–40%, 35–40% and 51.73% of hemicellulose, 18.9%, 30–50%, 40–45% and 51.73% of cellulose, 5.4%, 15–25%, 15% and 21.7% of lignin in *Musa acuminata* (MAC), *Cajanus cajan* (CCC), *Asclepias syriaca* floss (ASC) and *Pongamia pinnata* (PPC) respectively. During carbonization and chemical activation (using KOH), the hydrophilic & hydrophobic interaction of these macromolecules at high temperature changes which leads to the formation carbon skeletal structure with variations in its structural, morphological and surface properties [37].

The Raman spectroscopy was demonstrated to figure out structural properties of all four activated carbon materials derived from four different biomasses Fig. 1b. The Raman spectra of the activated carbon materials displayed D and G characteristic bands. The D band at  $\sim 1350\text{ cm}^{-1}$  ascribed to  $\text{sp}^3$  carbons, while G band at  $\sim 1550\text{ cm}^{-1}$  is due to in-plane vibration of  $\text{sp}^2$  carbon atoms [38]. From Raman spectral analysis of four different carbon materials indicated higher degree of defects formed (ID/IG ratio) as in the case of ASC (0.94) and CCC (0.99), than MAC (0.67) and PPC (0.79). The specific capacitance values of ASC and CCC were higher than MAC and PPC as discussed further in the text. This may be attributed to the number of defects formed would also influence microporous structure with almost similar pore volume and pore diameter. As observed in our previous study the presence of micropores provides high surface area for electrolyte ion adsorption and the presence of mesopores would lower resistance for movement of electrolyte ions. Hence, the presence of appropriate quantities of micro and mesoporous structure is required to establish higher specific capacitance value.

$\text{N}_2$  adsorption desorption analysis was performed to measure the porosity of synthesized activated carbon materials and the corresponding isotherms are provided in Fig. 1c. It can be observed from Fig. 1c, all the carbon materials exhibits type I isotherm according to IUPAC classification which indicates primarily microporous nature with indistinct hysteresis loop [38]. The surface area, total pore volume, mean pore diameter, micropore (MP plot & t-plot) and mesopore (Dollimore & Heal-DH plot, Carnston & Inkley-CI plot) diameter maxima,  $I_D/I_G$  ratio and specific capacitance values of all carbon materials are provided Table 1 (Fig. 1d). The large variation in the surface area values of KOH activated carbons are observed from Table 1 column 2. MAC exhibited highest surface area of  $3351\text{ m}^2/\text{g}$  and lowest by PPC as  $1260\text{ m}^2/\text{g}$  among the activated carbon samples. The material PPC possesses low pore volume and intermediate pore diameter with micro and meso pores. The same material also exhibited intermediate ID/IG ratio value compared to other carbon materials. Hence appropriate pore volume, pore diameter and the defects formed during chemical activation would definitely influence the electrochemical performance of these carbon materials. Here, it is also noteworthy to mention that, the interactions of KOH with carbon derived from various biomasses are correlated to its basic polymeric structure. Similarly, the other surface properties such as pore volume and pore diameters of activated carbon materials particularly fluctuates. In ASC the estimated values of BET surface area, total pore volume, mean pore diameter were moderate consisting of micropores and mesopores maxima around 0.6 and 10 nm respectively. The presence of such micropores would lead to high surface area for electrolyte ion and mesopores helps in offering low resistance for the movement of electrolyte ions [33]. Thus ASC has appropriate surface properties consisting of both micropores and mesopores on comparison with other activated carbons derived from biomass materials. Hence it's presumed that, the presence of such micro and mesopores in the activated carbon would definitely improve the EDLCs properties. It is critical to have an appropriate micro and mesoporous assembly for Helmholtz adsorption and desorption of the charges at the interface between the electrode surface and the electrolyte. This kind of observation was made in both ASC & PPC and further such mesoporous structure was not found in MAC and CCC samples. The evidence for slightly higher EDLC properties of ASC & PPC than MAC & CCC carbon materials are validated and described further in the text.

The SEM images of all the activated carbons are provided in Fig. 2(a–d). The morphology of MAC in Fig. 2a, appears to be agglomerated and distorted two dimensional opened tubes where as in PPC (Fig. 2b), different sized cavities are found only on the surface of carbon material. A clear morphology of the individual cavity of PPC with both micro and mesoporous structure has been provided as inset in Fig. 2b. CCC sample showed a three dimensional tunnel like porous structure with micropores after KOH activation process. The morphology of ASC appears to be opened tube like structure but unlike MAC, it is not in agglomerated state. Further tiny particles along with distorted tubes were also found contributing to micro and mesoporous nature. It is noteworthy that, all activated carbon materials attributes different morphology even though KOH is the common activation agent and synthesis conditions are same. This was presumed due to inherent surface properties of non-activated carbons possessing various macro/polymeric molecules. EDS spectrum of all the activated carbon materials indicated the presence of major components as carbon, oxygen and hydrogen along with inorganic trace elements. The presence of inorganic trace elements due to biomaterial itself may interact with carbon & oxygen to form

**Table 1**

Surface area, total pore volume, mean pore diameter, micropore and mesopore diameter maxima,  $I_D/I_G$  ratio and specific capacitance values of all carbon materials.

Sample name	Surface Area ( $\text{m}^2/\text{g}$ )	Total pore Volume ( $\text{cm}^3/\text{g}$ )	Mean pore Diameter (nm)	Micropore diameter (nm) maxima		Mesopore diameter (nm) maxima		$I_D/I_G$ ratio	Cs (F/g)
	BET plot	BET plot	BET Plot	MP plot	t-plot	DH plot	CI plot		
MAC	3351	1.99	2.37	1.10	1.37	–	–	0.67	358
PPC	1260	0.588	1.86	0.6	0.71	5	5	0.79	371
CCC	1583	0.71	1.79	0.8	0.74	–	–	0.99	343
ASC	1403	0.631	1.79	0.6	0.68	10	10	0.94	540



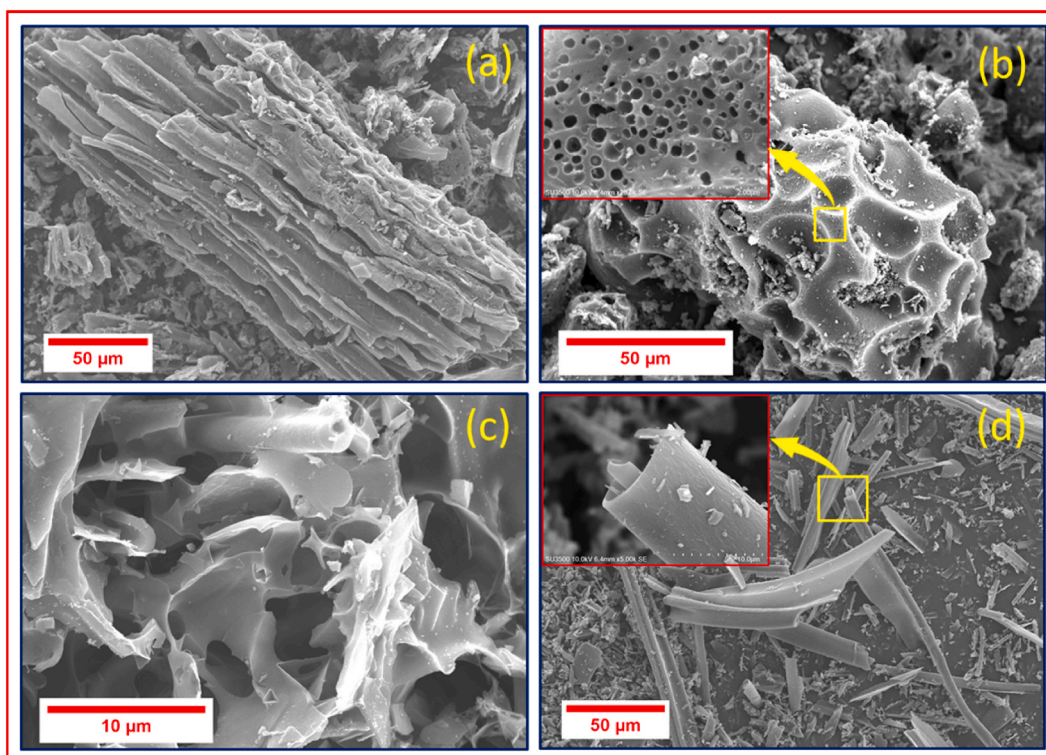


Fig. 2. SEM images of (a) MAC, (b) PPC, (c) CCC and (d) ASC carbon materials.

oxides & silicates [35].

### 3.2. Electrochemical studies of carbon materials in three electrode system

All the carbon materials were examined by CV, CP and EIS studies in three electrode configuration using 1 M KOH solution. Primarily, the electrodes were subjected to stabilization process for 30 cycles at a scan rate of 25 mV/s. Later on the electrodes were scanned at various scan rates from 2 to 500 mV/s at a fixed potential window. The operating potential windows in CV technique for individual ACs derived from four different biomass sources were found to be in the range MAC (−1.6 to 0.4 V), PPC (−1.6 to 0.2 V), CCC (−1.4 to 0.2 V) and ASC (−1.6 to 0.4 V). Fig. 3a depicts cyclic voltammogram patterns of the electrodes made by activated carbon from different biomasses at a scan rate of 10 mV/s and displayed rectangular shapes with negligible redox peaks validates ideal electric double layer capacitors behaviour [39,40]. The estimated specific capacitance values obtained for MAC, PPC, CCC & ASC are 358, 371, 343 & 540 F/g at scan rate of 2 mV/s respectively. Fig. 3b denotes the discrepancy of specific capacitance values as a function of scan rates for all the carbon materials. It is observed that, owing to the inadequate diffusion of active ions on the surface of electrode materials, the specific capacitance values decreases with increase in scan rates [11,41]. Amongst all the carbon materials, ASC

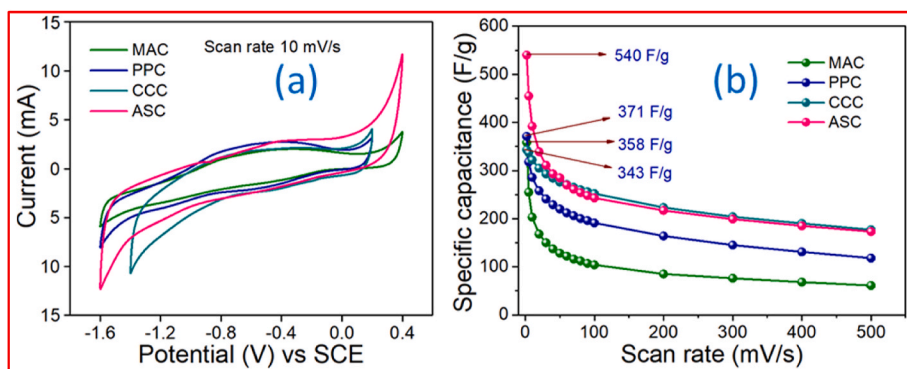


Fig. 3. (a) CV overlaid patterns at 10 mV/s (b) Specific capacitance against different scan rates from 2 to 500 mV/s for all the carbon materials.

exhibited high specific capacitance of 540 F/g & retained 45% Cs at 100 mV/s and 32% Cs at a scan rate of 500 mV/s, this is owing to tubular structure of activated carbon consisting of both micropore and mesopores which helps in easy transportation of electrolyte ions while charging and discharging process. Further high supercapacitance performance of ASC is also attributed to its high electrochemical active surface area. The electrochemical active surface area can be calculated using the below equation (1) [41].

$$SE = \frac{C_{dm}}{C_d} \quad (1)$$

where,  $C_{dm}$  is obtained from Nyquist plot at low frequency,  $C_d$  is constant value of  $20 \mu\text{Fcm}^{-2}$ . The estimated electrochemical active surface area ( $S_E$ ) of the different carbon materials MAC, PPC, CCC, ASC were found to be 355, 285, 395,  $480 \text{ m}^2 \text{ g}^{-1}$  [41]. However, the supercapacitance performance of carbon materials are not directly influenced by their BET surface area [40].

Galvanostatic charge discharge studies of all the carbon materials were carried out using chronopotentiometry technique at various current densities ranging from 2.5 to 50 A/g.

Fig. 4a represents the discharge curves at a current density of 10 A/g for all carbon materials. The potential window was different for all the activated carbons, however for ASC it was nearly  $-1.4$  to  $0.4$  V (1.8 V). As shown in Fig. 4a symmetrical triangular shape confirms capacitive reversibility and ideal electric double layer capacitance characteristics which is in consistent with CV results [42]. However, shape distortion can be observed in discharge curves of MAC, PPC, CCC which may be due to series of internal resistance, but in the case of ASC it would be less compare to others []. The specific capacitance values were calculated for different current densities for all the four carbon materials (Fig. 4b). Furthermore, the specific capacitance of MAC, PPC, CCC and ASC are in the following order 102, 235, 188 & 310 F/g at a current density of 2.5 A/g. ASC material has high specific capacitance (310 F/g) compare to other carbon materials, this is owing to the combined effect of conductivity and pore size distribution [43–45]. Other important parameters like energy density, power density, coulombic efficiency and capacitance retention were also calculated by this technique using standard equations.

The capacitive behaviour and resistances offered by activated carbon materials were investigated by another important tool-Electrochemical Impedance Spectroscopy (EIS). EIS measurements were carried out at an open circuit potential in the frequency range 10 mHz–100 kHz. Fig. 5a shows the estimated specific capacitance as a function of log of frequency. The specific capacitance of MAC, PPC, CCC & ASC obtained from EIS data at open circuit potential are 71, 57, 79 & 96 F/g respectively. Nyquist plots exhibited nearly straight line in lower frequency region for ASC and CCC materials and small semi arc in high frequency region thus signifying ideal capacitive behaviour (Fig. 5b). The diameter of the semi arc is directly related to charge transfer resistance which is obtained from resistance between electrode and current collector. The smaller diameter concludes that lower internal resistance exhibited by the activated carbon materials [44,46]. The solution resistance ( $R_s$ ) of all carbon materials obtained from Nyquist plot are 2.74, 2.25, 1.96 &  $1.72 \Omega$  for MAC, PPC, CCC & ASC respectively. Further, all the activated carbon materials were subjected to continuous 10 k charge discharge cycles at a current density of 15 A/g. These activated carbons from different biomass sources demonstrated a major change in cycles stability tests with respect to their capacitance retention, coulombic efficiency and number of charge discharge cycles as in Fig. 5c. The carbon materials MAC, PPC, CCC & ASC exhibited 3 k, 10 k, 5 k and 10 k cycles stability respectively with 100% coulombic efficiency. Cs retention of these carbon materials are provided at the end of Table 2. Among these carbon materials, ASC exhibited high cycle stability with 95% Cs retention and 100% coulombic efficiency at the end of 10 k cycles. Thus, ASC exhibited comparatively superior electrochemical performance than other biomass derived activated carbons by above mentioned three electroanalytical techniques.

### 3.3. Electrochemical studies of symmetric coin cell (ASC//ASC)

To ascertain the appropriate operating potential window of the symmetric coin cell using ASC, the cell was subjected to different potential windows from 0 to 1.2, 1.4, 1.6, 1.8 and 2 V at a fixed scan rate of 10 mV/s (Fig. 6a). The rectangular shaped CV patterns indicated pure EDLC behaviour of symmetric coin cell (ASC//ASC). Notably, larger area was observed for CV pattern of 0–2 V potential window. Hence in the same operating potential window, the CV patterns for various scan rates ranging from 2 to 500 mV/s were

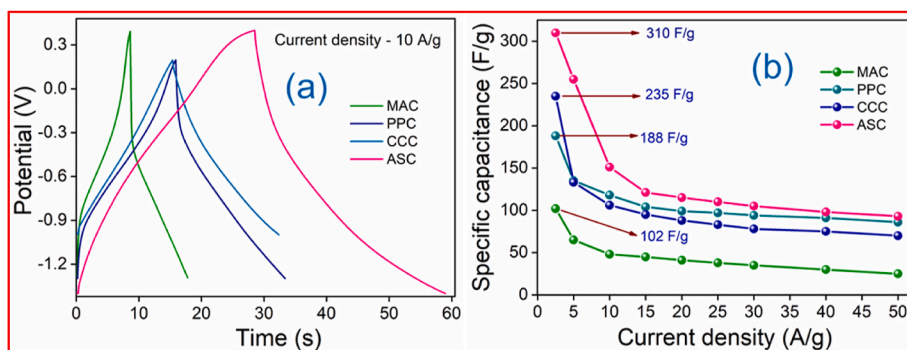
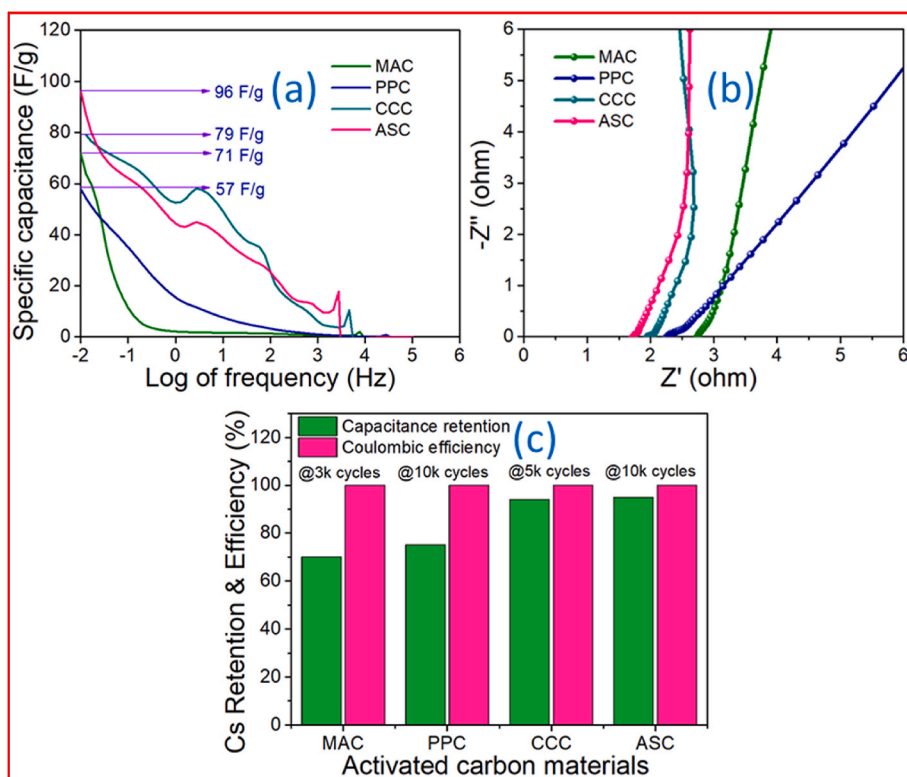


Fig. 4. (a) Discharge curves at 10 A/g (b) Specific capacitance versus different current densities from 2.5 to 50 A/g for all the carbon materials.



**Fig. 5.** (a) Estimated capacitance values against log of frequency from EIS study and (b) Nyquist plots (c) Cycles stability of MAC, PPC, CCC & ASC carbon materials.

**Table 2**

The EDLC performance of KOH activated carbons from derived various biomasses and in aqueous KOH electrolyte.

Biomass material	Surface area (m <sup>2</sup> /g)	Aqueous Electrolyte	Specific capacitance (F/g)	Current density (A/g)	Cs Retention % (Cycles)	Ref.
Rice husk	2696	6 M KOH	147	0.1	85 (10 k)	[36]
Walnut shell	1016	6 M KOH	169	0.5	94.6 (1 k)	[47]
Chinar fruit fluff	1758	6 M KOH	247	1.0	87.4 (10 k)	[48]
Sakura petals	1433	6 M KOH	265	0.2	90.2 (2 k)	[49]
Wild rice stem	1228	6 M KOH	301	1.0	98 (20 k)	[50]
Laminaria Japonica	1902	6 M KOH	192	0.1	100 (10 k)	[51]
Wheat-straw	1905	6 M KOH	306	1.0	93.9 (10 k)	[52]
Loofah sponge	2718	6 M KOH	309	1.0	81.3 (10 k)	[53]
Withered Rose	1911	6 M KOH	208	0.5	99 (25 k)	[54]
Walnut shells	724	6 M KOH	186	0.5	100 (20 k)	[55]
Litchi shell	1122	6 M KOH	222	0.1	97.3 (5 k)	[56]
Waste coffee grounds	1250	1 M KOH	105	0.5	133 (8 k)	[30]
Musa Acuminata stem (MAC)	3351	1 M KOH	102	2.5	70 (3 k)	This work
Pongamia pinnata seed oil extract cake (PPC)	1260	1 M KOH	235	2.5	74 (10 k)	This work
Cajanus Cajan stem (CCC)	1583	1 M KOH	188	2.5	93 (5 k)	This work
Asclepias syriaca floss (ASC)	1403	1 M KOH	310	2.5	95 (10 k)	This work

recorded (Fig. 6b). The coin cell exhibited a specific capacitance of 80 F/g at a scan rate of 2 mV/s, however the cell retained a Cs of 47 F/g at a scan rate of 100 mV/s with Cs retention of 59%. The decline in the Cs values at high scan rate was due to low adsorption/desorption rates at the interface between electrolyte and electrode surface. Galvanostatic charge-discharge cycles were carried out for the cell at various current densities range from 2.5 to 50 A/g in the potential window of 0–2 V. A symmetrical inverted V shaped CP curve of the cell implied the EDLC performance as provided in Fig. 6c. The coin cell exhibited Cs of 67 F/g at a current density of 2.5 A/g and also retained Cs of 29 F/g at 50 A/g (nearly 43% Cs retention). EIS studies were made for the coin cell to find out solution



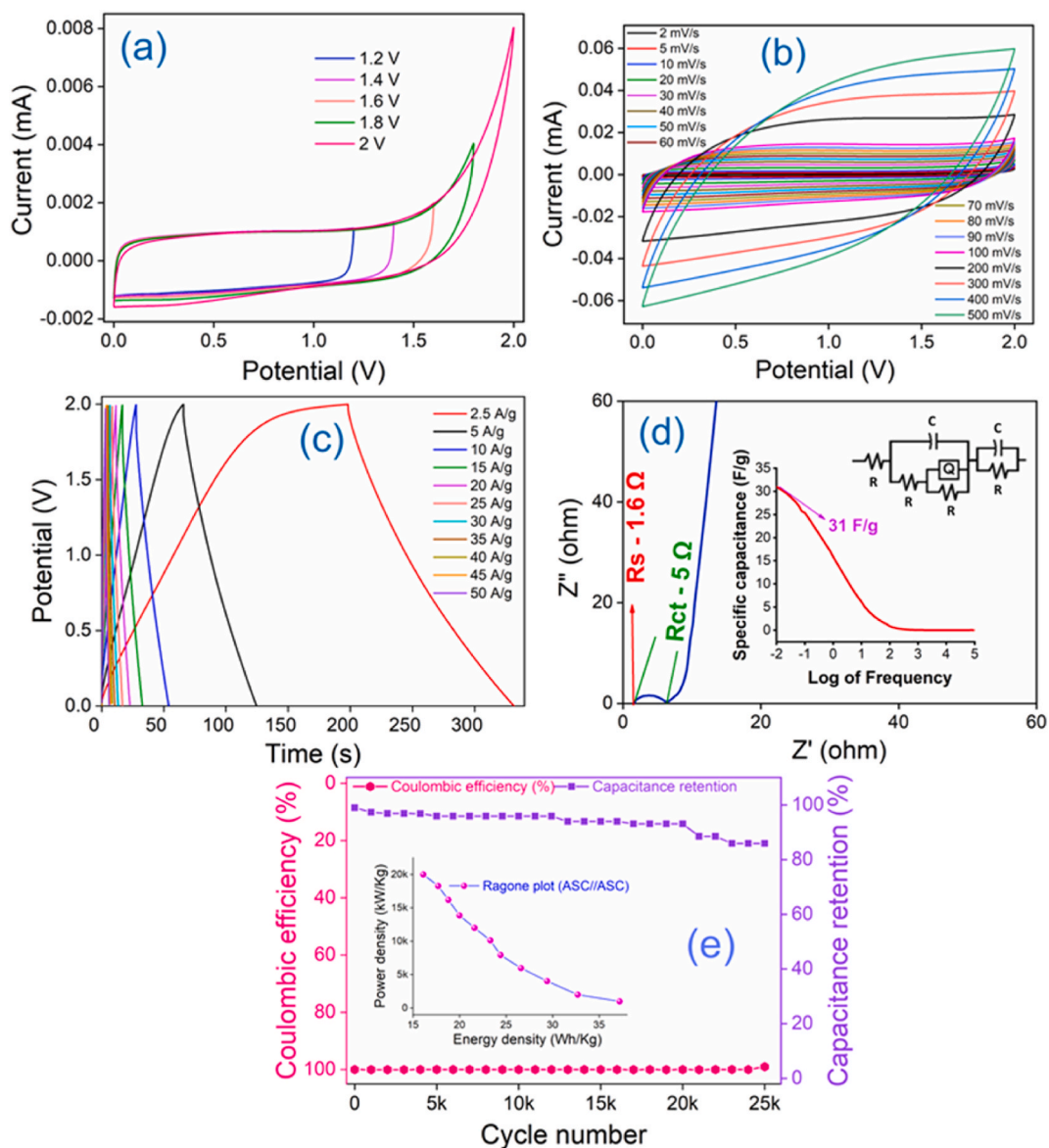


**Fig. 6.** (a) CV responses of the cell at various operating potential windows, (b) CV responses at different scan rates, (c) charge-discharge curves at different current densities, (d) Nyquist plot (Estimated Cs value obtained from EIS data and equivalent circuit as inset) & (e) Capacitance retention and coulombic efficiency for 25,000 cycles (Ragone plot for the cell as inset).

resistance ( $R_s$ ) and charge transfer resistance ( $R_{ct}$ ) to recognize the viability of the cell. These  $R_s$  and  $R_{ct}$  values were found to be 1.6 and 5  $\Omega$ . Nyquist plot and a plot of log of frequency Vs specific capacitance (bode plot as inset) are provided in Fig. 6d. Further, the Nyquist plot of device was fitted with an equivalent circuit using ZSimpWin 3.21 software and provided as inset in Fig. 6d. The estimated ED of the coin cell was found to be 37.2 W h/kg with a corresponding equivalent PD of 1 kW/kg and also retained 16.1 W h/kg at a maximum power density of 19.9 kW/kg (Fig. 6e-inset). The coin cell was subjected to 25,000 cycles stability at a high current density of 50 A/g. The cell indicated  $C_s$  retention of almost 86% with 100% coulombic efficiency (Fig. 6 (e)).

#### 4. Conclusion

In summary, the recycling of inexpensive widely available agricultural waste such as *Musa Acuminata* stem (MAC), *Pongamia pinnata* seed oil extract cake (PPC), *Cajanus Cajan* stem (CCC) and *Asclepias syriaca* floss (ASC) was employed to produce activated carbon using KOH as activation agent. The physico-chemical properties of all activated carbons were carefully analyzed using different analytical techniques and compared. Also, studied their electrochemical performances as EDLCs materials in three electrode system. Activated carbons derived from MAC, PPC, CCC and ASC exhibited a specific capacitance of 358, 343, 355 & 540 F/g at a scan rate of 2

mV/s and 102, 188, 253 & 256 F/g at a current density of 2.5 A/g. All the carbon materials exhibited 10 k cycles stability with a major difference in their cycles stability, coulombic efficiency and capacitance retention indicating the influence of morphological and surface properties. This is also attributed to the basic inherited polymeric constituents present in the biomass materials. The fabricated ASC//ASC also exhibited ED and PD of 37.2 W h/kg and 19.9 kW/kg with 25,000 cycles stability with reasonable Cs retention of 86% and 100% coulombic efficiency.

#### Author contribution statement

**Gopalakrishna Byatarayappa:** Conceived and designed the experiments; Performed the experiments.

**Radhika M G, Srilakshmi. R:** Performed the experiments; Analyzed and interpreted the data.

**Tejashree V, Krishna Venkatesh, Nagaraju N:** Analyzed and interpreted the data; Contributed reagents, materials, analysis tools or data.

**Kathyayini Nagaraju:** Analyzed and interpreted the data; Wrote the paper.

#### Data availability statement

Data will be made available on request.

#### Declaration of competing interest

The authors state that there are no known competing economic interests or personal relationships that may have influenced the work described in this paper.

#### Acknowledgement

All authors acknowledge the financially supported from Department of Science and Technology-Materials for Energy Storage (DST-MES) Ref No. DST/TMD/MES/2K17/02.

#### References

- [1] T. Adinaveen, L.J. Kennedy, J.J. Vijaya, G. Sekaran, Studies on structural, morphological, electrical and electrochemical properties of activated carbon prepared from sugarcane bagasse, *J. Ind. Eng. Chem.* 19 (2013) 1470–1476, <https://doi.org/10.1016/j.jiec.2013.01.010>.
- [2] A. Thambidurai, J.K. Lourdasamy, J.V. John, S. Ganesan, Preparation and electrochemical behaviour of biomass based porous carbons as electrodes for supercapacitors - a comparative investigation, *Kor. J. Chem. Eng.* 31 (2014) 268–275, <https://doi.org/10.1007/s11814-013-0228-z>.
- [3] T.A.L. John, K.J. Judith, G. Sekaran, Surface and porous characterization of activated carbon prepared from pyrolysis of biomass (rice straw) by two-stage procedure and its applications in supercapacitor electrodes, *J. Mater. Cycles Waste Manag.* 17 (2014) 736–747, <https://doi.org/10.1007/s10163-014-0302-6>.
- [4] Zijiong Li, Dongfang Guo, Yanyue Liu, Haiyan Wang, Lingli Wang, Recent advances and challenges in biomass-derived porous carbon nanomaterials for supercapacitors, *Chem. Eng. J.* 397 (2020), 125418, <https://doi.org/10.1016/j.cej.2020.125418>.
- [5] Z. Bi, Q. Kong, Y. Cao, G. Sun, F. Su, X. Wei, X. Li, A. Ahmad, L. Xie, C.M. Chen, Biomass-derived porous carbon materials with different dimensions for supercapacitor electrodes: a review, *J. Mater. Chem. A* 7 (2019) 16028–16045, <https://doi.org/10.1039/c9ta04436a>.
- [6] Poonam, K. Sharma, A. Arora, S.K. Tripathi, Review of supercapacitors: materials and devices, *J. Energy Storage* 21 (2019) 801–825, <https://doi.org/10.1016/j.est.2019.01.010>.
- [7] R. Kotz, M. Hahn, R. Gallay, Temperature behavior and impedance fundamentals of supercapacitors, *J. Power Sources* 154 (2006) 550–555, <https://doi.org/10.1016/j.jpowsour.2005.10.048>.
- [8] Z. Li, D. Guo, Y. Liu, H. Wang, L. Wang, Recent advances and challenges in biomass-derived porous carbon nanomaterials for supercapacitors, *Chem. Eng. J.* 397 (2020), 125418, <https://doi.org/10.1016/j.cej.2020.125418>.
- [9] A. Muzaffar, M.B. Ahamed, K. Deshmukh, J. Thirumalai, A review on recent advances in hybrid supercapacitors: design, fabrication and applications, *Renew. Sustain. Energy Rev.* 101 (2019) 123–145, <https://doi.org/10.1016/j.rser.2018.10.026>.
- [10] M.G. Radhika, G. Byatarayappa, D. V Ingale, L. Kudinalli, G. Bhatta, K. Venkatesh, S.K.M.K. Nagaraju, High performance of asymmetric coin cells designed using optimized weight percentage of multiwalled carbon nanotubes in Ni/Co-MOFs nanocomposites, *Mater. Res. Bull.* 156 (2022), 111996, <https://doi.org/10.1016/j.materresbull.2022.111996>.
- [11] B. Gopalakrishna, N. Nagaraju, K. Venkatesh, D. Xiao, N. Kathyayini, Studies on the influence of weight percentage of multiwalled carbon nanotubes in Mn/Ni/Co nanocomposites for hybrid supercapacitors, *Inorg. Chem. Commun.* 124 (2021), 108371, <https://doi.org/10.1016/j.inoche.2020.108371>.
- [12] L. Thomas, S. Pete, K. Chaitra, K. Venkatesh, B. Gopalakrishna, K. Nagaraju, Facile synthesis of PANI-MWCNT-Ni(OH)<sub>2</sub> ternary composites and study of their performance as electrode material for supercapacitors, *Diam. Relat. Mater.* 106 (2020), 107853, <https://doi.org/10.1016/j.diamond.2020.107853>.
- [13] M.G. Radhika, B. Gopalakrishna, K. Chaitra, L.K.G. Bhatta, K. Venkatesh, M.K. Sudha Kamath, N. Kathyayini, Electrochemical studies on Ni, Co & Ni/Co-MOFs for high-performance hybrid supercapacitors, *Mater. Res. Express* 7 (2020), 054003, <https://doi.org/10.1088/2053-1591/ab8d5d>.
- [14] Xin Zhang, et al., Sulfur vacancies-induced 'Electron bridge' in Ni<sub>4</sub>MO/sv-Zn CD1-s regulates Electron transfer for efficient H<sub>2</sub>-releasing photocatalysis, *J. Energy Chem.* 79 (2023) 64–71, <https://doi.org/10.1016/j.jechem.2023.01.001>.
- [15] Xin Guo, et al., Engineering Electron redistribution of bimetallic phosphates with CEO<sub>2</sub> enables high-performance overall water splitting, *Chem. Eng. J.* 453 (2023), 139796, <https://doi.org/10.1016/j.cej.2022.139796>.
- [16] Manyi Gao, et al., Mutual-modification effect in adjacent Pt nanoparticles and single atoms with sub-nanometer inter-site distances to boost photocatalytic hydrogen evolution, *Chem. Eng. J.* 446 (2022), 137127, <https://doi.org/10.1016/j.cej.2022.137127>.
- [17] Xin Guo, et al., Hierarchical core-shell electrode with Ni<sub>2</sub>O<sub>4</sub> nanoparticles wrapped MnCO<sub>2</sub>O<sub>4</sub> nanowire arrays on Ni foam for high-performance asymmetric supercapacitors, *J. Colloid Interface Sci.* 563 (2020) 405–413, <https://doi.org/10.1016/j.jcis.2019.12.076>.
- [18] Fengyu Wu, et al., O and n Co-doped porous carbon derived from crop waste for a high-stability all-solid-state symmetric supercapacitor, *New J. Chem.* 46 (41) (2022) 19667–19674, <https://doi.org/10.1039/d2nj04125a>.
- [19] K. Chaitra, N. Nagaraju, Kathyayini Nagaraju, Nanocomposite of hexagonal β-Ni(OH)<sub>2</sub>/Multiwalled carbon nanotubes as high performance electrode for hybrid supercapacitors, *Mater. Chem. Phys.* 164 (2015) 98–107.

- [20] G. Zhang, Y. Chen, Y. Chen, H. Guo, Activated biomass carbon made from bamboo as electrode material for supercapacitors, *Mater. Res. Bull.* 102 (2018) 391–398, <https://doi.org/10.1016/j.materresbull.2018.03.006>.
- [21] M. Li, H. Xiao, T. Zhang, Q. Li, Y. Zhao, Activated carbon fiber derived from sisal with large specific surface area for high-performance supercapacitors, *ACS Sustain. Chem. Eng.* 7 (2019) 4716–4723, <https://doi.org/10.1021/acsschemeng.8b04607>.
- [22] J. Elisadiki, T.E. Kibona, R.L. Machunda, M.W. Saleem, W.S. Kim, Y.A.C. Jande, Biomass-based carbon electrode materials for capacitive deionization: a review, *Biomass Convers. Biorefinery*. 10 (2020) 1327–1356, <https://doi.org/10.1007/s13399-019-00463-9>.
- [23] J.R. Rajabathar, M. Sivachidambaram, J.J. Vijaya, H.A. Al-lohedan, D.M.D. Aldhayan, Flexible type symmetric supercapacitor electrode fabrication using phosphoric acid-activated carbon nanomaterials derived from cow dung for renewable energy applications, *ACS Omega* 25 (2020) 15028–15038, <https://doi.org/10.1021/acsomega.0c00848>.
- [24] R. Jothi, M. Sivachidambaram, J.J. Vijaya, H.A. Al-lohedan, M.R. Muthumareeswaran, Biomass and Bioenergy Synthesis of porous activated carbon powder formation from fruit peel and cow dung waste for modified electrode fabrication and application, *Biomass Bioenergy* 142 (2020), 105800, <https://doi.org/10.1016/j.biombioe.2020.105800>.
- [25] Majid Shaker, et al., Biomass-derived porous carbons as supercapacitor electrodes – a review, *N. Carbon Mater.* 36 (3) (2021) 546–572, [https://doi.org/10.1016/s1872-5805\(21\)60038-0](https://doi.org/10.1016/s1872-5805(21)60038-0).
- [26] Binoy K. Saikia, et al., A brief review on supercapacitor energy storage devices and utilization of natural carbon resources as their electrode materials, *Fuel* 282 (2020), 118796, <https://doi.org/10.1016/j.fuel.2020.118796>.
- [27] Shashank Sundriyal, et al., Advances in bio-waste derived activated carbon for supercapacitors: trends, challenges and prospective, *Resour. Conserv. Recycl.* 169 (2021), 105548, <https://doi.org/10.1016/j.resconrec.2021.105548>.
- [28] Y. Gao, Q. Yue, B. Gao, A. Li, Insight into activated carbon from different kinds of chemical activating agents: a review, *Sci. Total Environ.* 746 (2020), 141094, <https://doi.org/10.1016/j.scitotenv.2020.141094>.
- [29] M. Hunsom, C. Authanit, Adsorptive purification of crude glycerol by sewage sludge-derived activated carbon prepared by chemical activation with H<sub>3</sub>PO<sub>4</sub>, K<sub>2</sub>CO<sub>3</sub> and KOH, *Chem. Eng. J.* 229 (2013) 334–343, <https://doi.org/10.1016/j.cej.2013.05.120>.
- [30] Y.H. Chiu, L.Y. Lin, Effect of activating agents for producing activated carbon using a facile one-step synthesis with waste coffee grounds for symmetric supercapacitors, *J. Taiwan Inst. Chem. Eng.* 101 (2019) 177–185, <https://doi.org/10.1016/j.jtice.2019.04.050>.
- [31] A.S. Mestre, C. Freire, J. Pires, A.P. Carvalho, M.L. Pinto, High performance microspherical activated carbons for methane storage and landfill gas or biogas upgrade, *J. Mater. Chem. A* 2 (2014) 15337–15344, <https://doi.org/10.1039/c4ta03242j>.
- [32] G. Byatarayappa, V. Guna, K. Venkatesh, N. Reddy, N. Nagaraju, K. Nagaraju, Superior cycle stability performance of a symmetric coin cell fabricated using KOH activated bio-char derived from agricultural waste – Cajanus cajan stems, *J. Environ. Chem. Eng.* 9 (2021), 106525, <https://doi.org/10.1016/j.jece.2021.106525>.
- [33] K. Chaitra, R. Narendra, K. Venkatesh, N. Nagaraju, N. Kathyayini, Green " carbon with hierarchical three dimensional porous structure derived from - Pongamia pinnata seed oil extract cake and NiCo<sub>2</sub>O<sub>4</sub> - Ni(OH)<sub>2</sub>/Multiwall carbon nanotubes nanocomposite as electrode materials for high performance asymmetric supe, *J. Power Sources* 356 (2017) 212–222, <https://doi.org/10.1016/j.jpowsour.2017.04.085>.
- [34] K. Chaitra, T.R. Vinny, P. Sivaraman, N. Reddy, C. Hu, K. Venkatesh, S.C. Vivek, N. Nagaraju, N. Kathyayini, KOH activated carbon derived from biomass-banana fibers as an efficient negative electrode in high performance asymmetric supercapacitor, *J. Energy Chem.* 26 (2017) 56–62, <https://doi.org/10.1016/j.jechem.2016.07.003>.
- [35] G. Byatarayappa, U.M. Bhatta, D.V. Ingale, K. Venkatesh, N.N.K. Nagaraju, A correlation of surface/textural properties of carbon derived from Musa acuminata stem and its high supercapacitance performance with superior cycle stability, *J. Energy Storage* 44 (2021), 103424, <https://doi.org/10.1016/j.est.2021.103424>.
- [36] L. Wan, D. Chen, J. Liu, Y. Zhang, J. Chen, C. Du, M. Xie, Facile preparation of porous carbons derived from orange peel via basic copper carbonate activation for supercapacitors, *J. Alloys Compd.* 823 (2020), 153747, <https://doi.org/10.1016/j.jallcom.2020.153747>.
- [37] A. Jain, R. Balasubramanian, M.P. Srinivasan, Hydrothermal conversion of biomass waste to activated carbon with high porosity: a review, *Chem. Eng. J.* 283 (2016) 789–805, <https://doi.org/10.1016/j.cej.2015.08.014>.
- [38] E.Y.L. Teo, L. Muniandy, E.P. Ng, F. Adam, A.R. Mohamed, R. Jose, K.F. Chong, High surface area activated carbon from rice husk as a high performance supercapacitor electrode, *Electrochim. Acta* 192 (2016) 110–119, <https://doi.org/10.1016/j.electacta.2016.01.140>.
- [39] M.J.P. Brito, C.M. Veloso, L.S. Santos, R.C.F. Bonomo, R. da C.I. Fontan, Adsorption of the textile dye Dianix® royal blue CC onto carbons obtained from yellow mombin fruit stones and activated with KOH and H<sub>3</sub>PO<sub>4</sub>: kinetics, adsorption equilibrium and thermodynamic studies, *Powder Technol.* 339 (2018) 334–343, <https://doi.org/10.1016/j.powtec.2018.08.017>.
- [40] S. Li, K. Han, J. Li, M. Li, C. Lu, Preparation and characterization of super activated carbon produced from gulfweed by KOH activation, *Microporous Mesoporous Mater.* 243 (2017) 291–300, <https://doi.org/10.1016/j.micromeso.2017.02.052>.
- [41] Gomaa A.M. Ali, Mashitah M. Yusoff, Essam R. Shaaban, Kwok Feng Chong, High performance MnO<sub>2</sub> nanoflower supercapacitor electrode by electrochemical recycling of spent batteries, *Ceram. Int.* 43 (11) (2017) 8440, <https://doi.org/10.1016/j.ceramint.2017.03.195>, 48.
- [42] C.J. Raj, R. Manikandan, M. Rajesh, P. Sivakumar, H. Jung, S.J. Das, B.C. Kim, Cornhusk mesoporous activated carbon electrodes and seawater electrolyte: the sustainable sources for assembling retainable supercapacitor module, *J. Power Sources* 490 (2021), 229518, <https://doi.org/10.1016/j.jpowsour.2021.229518>.
- [43] K. Wang, N. Zhao, S. Lei, R. Yan, X. Tian, J. Wang, Y. Song, D. Xu, Q. Guo, L. Liu, Promising biomass-based activated carbons derived from willow catkins for high performance supercapacitors, *Electrochim. Acta* 166 (2015) 1–11, <https://doi.org/10.1016/j.electacta.2015.03.048>.
- [44] A. Wang, K. Sun, R. Xu, Y. Sun, J. Jiang, Cleanly synthesizing rotten potato-based activated carbon for supercapacitor by self-catalytic activation, *J. Clean. Prod.* 283 (2021), 125385, <https://doi.org/10.1016/j.jclepro.2020.125385>.
- [45] R. Farzana, R. Rajarao, B.R. Bhat, V. Sahajwalla, Performance of an activated carbon supercapacitor electrode synthesised from waste Compact Discs (CDs), *J. Ind. Eng. Chem.* 65 (2018) 387–396, <https://doi.org/10.1016/j.jiec.2018.05.011>.
- [46] J. Phiri, J. Dou, T. Vuorinen, P.A.C. Gane, T.C. Maloney, Highly porous willow wood-derived activated carbon for high-performance supercapacitor electrodes, *ACS Omega* 4 (2019) 18108–18117, <https://doi.org/10.1021/acsomega.9b01977>.
- [47] D. Lan, M. Chen, Y. Liu, Q. Liang, W. Tu, Y. Chen, J. Liang, F. Qiu, Preparation and characterization of high value-added activated carbon derived from biowaste walnut shell by KOH activation for supercapacitor electrode, *J. Mater. Sci. Mater. Electron.* 31 (2020) 18541–18553, <https://doi.org/10.1007/s10854-020-04398-0>.
- [48] Y. Zhao, J. Yang, X.Y. Wang, X.C. Zheng, Chinar fruit fluff-derived mesopore-dominant hierarchical porous carbon for high-performance supercapacitors, *J. Mater. Sci. Mater. Electron.* 32 (2021) 3498–3511, <https://doi.org/10.1007/s10854-020-05096-7>.
- [49] F. Ma, S. Ding, H. Ren, Y. Liu, Sakura-based activated carbon preparation and its performance in supercapacitor applications, *RSC Adv.* 9 (2019) 2474–2483, <https://doi.org/10.1039/c8ra09685f>.
- [50] Q. Tian, X. Wang, X. Xu, M. Zhang, L. Wang, X. Zhao, Z. An, H. Yao, J. Gao, A novel porous carbon material made from wild rice stem and its application in supercapacitors, *Mater. Chem. Phys.* 213 (2018) 267–276, <https://doi.org/10.1016/j.matchemphys.2018.04.026>.
- [51] Y. Cheng, L. Wu, C. Fang, T. Li, J. Chen, M. Yang, Q. Zhang, Synthesis of porous carbon materials derived from laminaria japonica via simple carbonization and activation for supercapacitors, *J. Mater. Res. Technol.* 9 (2020) 3261–3271, <https://doi.org/10.1016/j.jmrt.2020.01.022>.
- [52] W. Chen, X. Wang, C. Liu, M. Luo, P. Yang, X. Zhou, Rapid single-step synthesis of porous carbon from an agricultural waste for energy storage application, *Waste Manag.* 102 (2020) 330–339, <https://doi.org/10.1016/j.wasman.2019.10.058>.
- [53] X.L. Su, J.R. Chen, G.P. Zheng, J.H. Yang, X.X. Guan, P. Liu, X.C. Zheng, Three-dimensional porous activated carbon derived from loofah sponge biomass for supercapacitor applications, *Appl. Surf. Sci.* 436 (2018) 327–336, <https://doi.org/10.1016/j.apsusc.2017.11.249>.

- [54] C. Zhao, Y. Huang, C. Zhao, X. Shao, Z. Zhu, Rose-derived 3D carbon nanosheets for high cyclability and extended voltage supercapacitors, *Electrochim. Acta* 291 (2018) 287–296, <https://doi.org/10.1016/j.electacta.2018.09.136>.
- [55] H. Yang, Y. Tang, X. Huang, L. Wang, Q. Zhang, Activated porous carbon derived from walnut shells with promising material properties for supercapacitors, *J. Mater. Sci. Mater. Electron.* 28 (2017) 18637–18645, <https://doi.org/10.1007/s10854-017-7813-6>.
- [56] N. Zhao, P. Zhang, D. Luo, W. Xiao, L. Deng, F. Qiao, Direct production of porous carbon nanosheets/particle composites from wasted litchi shell for supercapacitors, *J. Alloys Compd.* 788 (2019) 677–684, <https://doi.org/10.1016/j.jallcom.2019.02.304>.